

Structure of Sodium Borosilicate Glasses: Models and Experiment

A. A. Osipov^{a,*} and L. M. Osipova^a

^a South Ural Federal Scientific Center for Mineralogy and Geoecology, Ural Branch, Russian Academy of Sciences, Ilmensky Reserve, Miass, 456317 Russia

*e-mail: armenakosipov32@gmail.com

Received June 2, 2022; revised July 11, 2022; accepted August 5, 2022

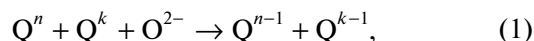
Abstract—This study is aimed at the analysis of two structural models of the structure of sodium borosilicate glasses (the Dell model and the thermodynamic (TD) model), which differ significantly in their fundamental principles. Where it is possible, we compare the model's predictions regarding the structural features of glasses in the Na₂O–B₂O₃–SiO₂ system on the near (distribution of basic structural units) and average (the content of superstructural groups as a function of glass composition) scales with the experimental data. The analysis gives an idea of the information content of both models and their correctness in terms of their predictions.

Keywords: borosilicate glasses, Dell model, thermodynamic model, basic structural units, superstructural groupings

DOI: 10.1134/S1087659622600521

INTRODUCTION

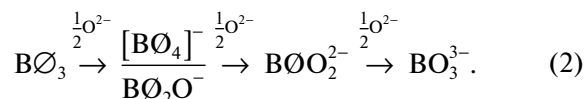
The study of the structure and properties of borosilicate glasses has a long history. Interest in these glasses is due, on the one hand, to their widespread use and the potential for the further expansion of their field of application in various industries, and, on the other hand, on the complexity of the structure, which is largely determined by the presence of two glass-forming oxides, SiO₂ and B₂O₃, each of whose cations form their own structural units. Silicate structural units are known to be SiO₄ tetrahedrons that differ in the number of bridging oxygen atoms. In the literature, these tetrahedra are also known as Qⁿ units, where *n* is the number of bridging oxygen atoms belonging to the given tetrahedron. Because the *n* can take values from 4 (fully polymerized Q⁴ structural units) to 0 (completely depolymerized Q⁰ units), five types of silicate tetrahedra are distinguished in total, and the modification of the local structure of the silicate network upon interaction with a modifier oxide can generally be represented as the following reaction:



where O²⁻ is the additional oxygen introduced into the system in the form of modifying oxides. This reaction implies that as a result of such an interaction the bridge bond between the two structural units breaks and two terminal (nonbridging) oxygen atoms are formed.

As for the borate structural groups, here, as in the previous case, it is customary to distinguish the five basic units: the symmetrical triangle BØ₃ (Ø is a bridg-

ing oxygen atom), in which all three oxygen atoms are bridging atoms, the tetrahedron [BØ₄]⁻, where all four oxygen atoms are also bridging atoms and there are three more trigonal borate units, differing in the number of bridging oxygen atoms—the metaborate triangle BØ₂O⁻, pyroborate unit BØO₂²⁻, and the fully depolymerized orthoborate anion BO₃³⁻. The modification of the boron–oxygen framework differs from that characteristic of the silicon–oxygen network, and this is due to the fact that the oxygen coordination number of boron atoms can change when a typical modifier oxide is added to B₂O₃. For example, in binary alkaline borate systems, such a sequence can be expressed as follows:



It should be clarified that although sequence (2) indicates the possibility of transforming symmetrical triangles BØ₃ as in tetrahedra [BØ₄]⁻ and into asymmetric metaborate units BØ₂O⁻, in fact, with the addition of an oxide-modifier of up to approximately 25–30 mol %, there is mainly a transformation of symmetrical triangles into BO₄ tetrahedra, and the appearance in the glass structure of trigonal borate units with different numbers of nonbridging oxygen atoms begins only at higher concentrations of the modifying oxide.

Another specific structural feature of the structure of borate glasses is the presence in them of the so-called superstructural groups, which consist of a cer-

Table 1. Mathematical formalism of the Dell model

Range			
I	II	III	IV
$0 \leq R \leq R_{\max}$	$R_{\max} \leq R \leq R_{d1}$	$R_{d1} \leq R \leq R_{d2}$	$R_{d2} \leq R \leq R_{d3}$
$N_4 = R$	$N_4 = R_{\max}$	$N_4 = (8 + K) \left(\frac{1}{12} - \frac{R}{24 + 12K} \right)$	$N_4 = (8 + K) \left(\frac{1}{12} - \frac{R}{24 + 12K} \right)$
$N_{3s} = 1 - R$	$N_{3s} = 1 - R_{\max}$	$N_{3s} = \left(1 - \frac{1}{8}K \right) \left(\frac{3}{4} - \frac{R}{2 + K} \right)$	$N_{3s} = 0$
$N_{3a} = 0$	$N_{3a} = 0$	$N_{3a} = \frac{1}{3}(R - R_{d1}) \left(\frac{2 - \frac{1}{4}K}{2 + K} \right)$	$N_{3a} = \left(\frac{4}{3} - \frac{1}{6}K \right) \left(1 - \frac{R}{2 + K} \right)$
$N_p = 0$	$N_{3p} = 0$	$N_p = \frac{1}{2}(R - R_{d1}) \left(\frac{2 - \frac{1}{4}K}{2 + K} \right) + \frac{2}{3} \left(\frac{KR}{8 + 4K} - \frac{K}{16} \right)$	$N_p = \frac{1}{2} \left(1 - \frac{1}{8}K \right) + (R - R_{d2}) \left(\frac{2 - \frac{1}{4}K}{2 + K} \right) + \frac{2}{15} \left(\frac{5KR}{8 + 4K} - \frac{5K}{16} \right)$
Limit values of parameter R			
$R_{\max} = \frac{1}{2} + \frac{1}{16}K, \quad R_{d1} = \frac{1}{2} + \frac{1}{4}K, \quad R_{d2} = \frac{3}{2} + \frac{3}{4}K, \quad R_{d3} = 2 + K$			

tain number of basic structural units strictly oriented relative to each other [1, 2]. Examples of such superstructural units are boroxol $B_3O_3O_3^-$ rings, triborate $B_3O_3O_4^-$ rings, pentaborate $B_5O_6O_4^-$ and diborate $B_4O_5O_4^{2-}$ groups, a metaborate $B_3O_6^{3-}$ ring anion, etc. It is logical to expect that such groups can also be present in borosilicate glass, and their concentration should be high in glasses with a low SiO_2 content. In addition, the formation of bridging oxygen bonds between borate and silicate structural units leads to the fact that, in addition to superstructural groups typical of pure borate systems, mixed ring groups, such as danburite or reedmergnerite rings, can also form in borosilicate glasses. Both types of rings, danburite or reedmergnerite, consist of four tetrahedrally coordinated structural units, only in the first case the ring is formed from two SiO_4 tetrahedra and two $[BO_4]^-$ tetrahedra, and in the second, the ring contains three SiO_4 tetrahedra and one borate tetrahedron.

Thus, the description of the structure of borosilicate glasses requires, in the most general case, the identification of ten types of structural units (five silicate and five borate) and the determination of their concentrations as a function of the glass composition and/or external parameters (for example, pressure or temperature), as well as the type and concentrations of larger superstructural groups (including mixed rings) that can form in the glass. It is obvious that changes in the concentration of silicate or borate structural units and the formation patterns of superstructural groups in the glass structure are determined by the distribution of the modifying oxide between the silicate and borate components of the borosilicate glass net-

work and the corresponding mechanisms of their modification.

Significant efforts have been made in studying these issues, in particular, the structure of glasses of the $Na_2O-B_2O_3-SiO_2$ system. The logical generalization of such works was the development of a number of structural models that differ significantly in their fundamental principles. The aim of this study is to analyze two well-known models in terms of the amount of information they provide, as well as the extent to which their predictions are correct.

DELL MODEL

Historically, one of the first models of the structure of sodium borosilicate glasses is the semiempirical Dell model [3, 4], which is based on a set of experimental data on the modification of the borate component of the sodium borosilicate glass network accumulated by the end of the 1970s and the beginning of the 1980s. In this model, the glass compositions are expressed in terms of oxide concentration ratios, $R = [Na_2O]/[B_2O_3]$ and $K = [SiO_2]/[B_2O_3]$, and each section with a constant value of parameter K divided into four ranges depending on the value of parameter R . Thus, to calculate the concentrations of borate structural units, a specific set of equations is used for each range (see Table 1). It makes sense to emphasize that such calculations result in the local distribution of borate structural units; i.e., the concentrations of borate units are calculated in relation to the total number of boron atoms in the system, and not in relation to the number of all network-forming cations.

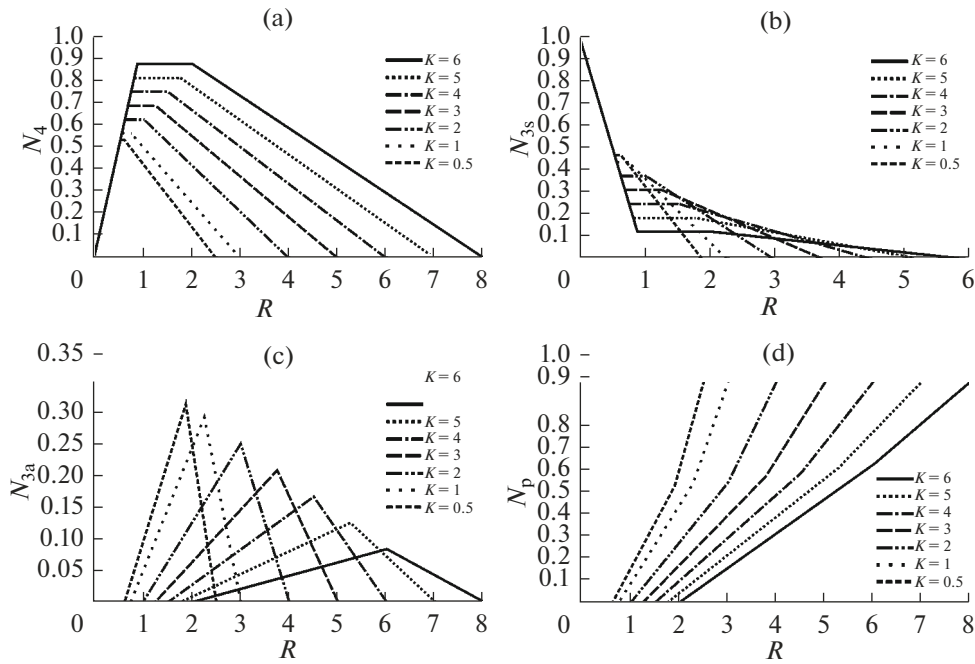


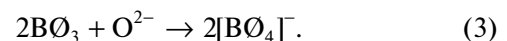
Fig. 1. Concentrations of borate structural units (local distribution) in glasses of the $\text{Na}_2\text{O}-\text{B}_2\text{O}_3-\text{SiO}_2$ system of sections with $K = 0.5, 1, 2, 3, 4, 5,$ and 6 (Dell model). Concentrations $[\text{B}\text{O}_4]^-$, BO_3 , $\text{B}\text{O}_2\text{O}^-$, and $\text{B}\text{O}\text{O}_2^{2-}$ units are designated as N_4 , N_{3s} , N_{3a} , and N_p , respectively.

Figure 1 shows the results of calculating the concentrations of borate structural units, N_4 ($[\text{B}\text{O}_4]^-$), N_{3s} (BO_3), N_{3a} ($\text{B}\text{O}_2\text{O}^-$), and N_{3p} ($\text{B}\text{O}\text{O}_2^{2-}$), for 7 sections with $K = 0.5, 1, 2, 3, 4, 5,$ and 6 . According to the model in the first range, all of the sodium oxide interacts only with the borate component of the borosilicate glass network, and the only result of such an interaction is the transformation of symmetrical borate triangles into borate tetrahedra. Therefore, regardless of the value of parameter K , an increase in the proportion of borate tetrahedra is described by the same straight line. The same is true for the proportion of symmetrical triangles, since no other borate structural units are formed in this range; i.e., the concentration of metaborate $\text{B}\text{O}_2\text{O}^-$ triangles and pyroborate $\text{B}\text{O}\text{O}_2^{2-}$ units is zero here. As the value of parameter K increases (with the increasing concentration of SiO_2 in the system), the width of the first range increases and the maximum possible concentration of borate tetrahedra for the given K increases.

In the second section, no changes take place in the concentrations of borate structural units. Here it is assumed that the entire oxide modifier interacts only with the silicate component of borosilicate glass. In the third and fourth ranges, the model assumes a proportional distribution of the modifying oxide between silicate and borate structural units, and in each section with a constant value of K , the decrease in the propor-

tion of borate tetrahedra is described by the same expression (see Table 1). Therefore, we cannot visually highlight the border between the third and fourth ranges on the dependence of the concentration of borate tetrahedra on the value of parameter R . As for the concentration of symmetrical triangles BO_3 , their fraction in the local distribution monotonically decreases to zero in the third range, and in the fourth range, and according to the Dell model, symmetrical borate triangles are absent in the structure of borosilicate glasses. The concentration of metaborate asymmetric triangles $\text{B}\text{O}_2\text{O}^-$ increases in the third range and reaches its maximum value at $R = R_{d2}$, and in the fourth, on the contrary, it decreases to zero. As for pyroborate $\text{B}\text{O}\text{O}_2^{2-}$ units, their concentration increases both in the third and fourth ranges. We note that the increment in the proportion of pyroborate units in the third range is somewhat less than in the fourth. As the value of K grows, this difference in the magnitude of the increment gradually decreases.

Thus, according to the Dell model, the transformation of the local structure of the borate component of the disordered network of borosilicate glass in different ranges is determined by different mechanisms. Namely, in range I, the modification of the structure at the level of basic structural units is described solely by the reaction



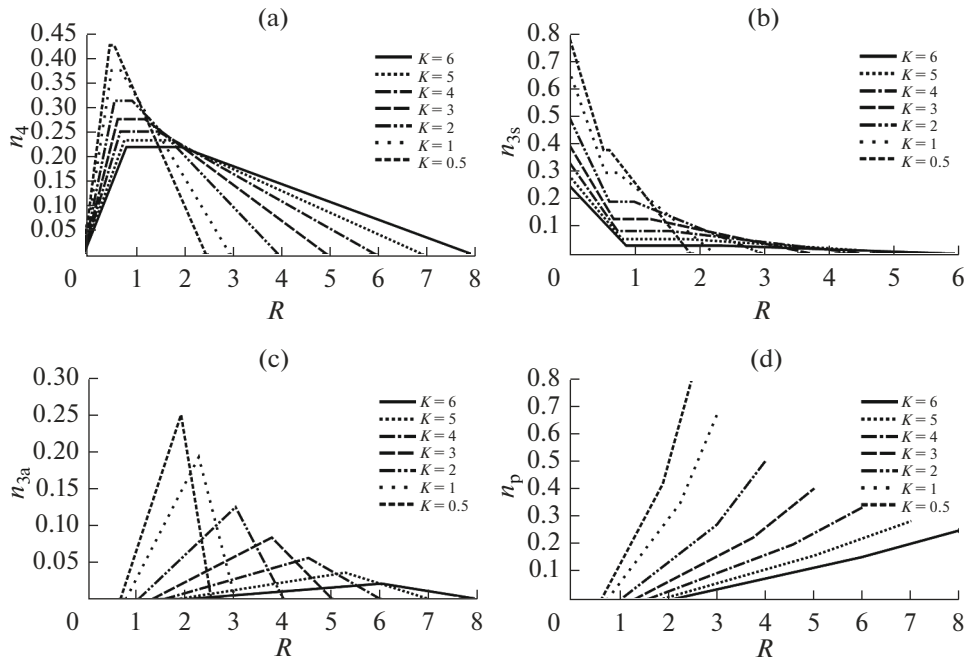
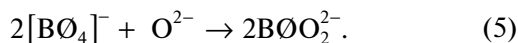
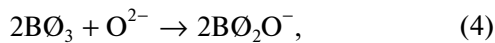


Fig. 2. Concentrations of borate structural units (general distribution) in glasses of the $\text{Na}_2\text{O}-\text{B}_2\text{O}_3-\text{SiO}_2$ system of sections with $K = 0.5, 1, 2, 3, 4, 5,$ and 6 (Dell model). Concentrations of $[\text{B}\text{O}_4]^-$, BO_3 , $\text{B}\text{O}_2\text{O}^-$, and $\text{B}\text{O}\text{O}_2^{2-}$ units are designated as n_4 , n_{3s} , n_{3a} , and n_p , respectively.

As noted above, in range II, out of the entire variety of basic borate structural units in glass, only fully polymerized symmetrical triangles BO_3 and tetrahedra $[\text{B}\text{O}_4]^-$ are present, while the concentrations of other borate units are zero. Moreover, within the second range, no changes occur in the distribution of borate units.

In range III, the model predicts an increase in the proportion of meta- ($\text{B}\text{O}_2\text{O}^-$) and pyroborate ($\text{B}\text{O}\text{O}_2^{2-}$) units against the background of a decrease in the proportion of symmetrical triangles and borate tetrahedra. The proportion of metaborate asymmetric triangles at the end of this range reaches its maximum value in all sections with the fixed K parameter, and the proportion of symmetrical triangles becomes zero. Obviously, here the modification of the local structure can be expressed in the form of two simultaneously occurring reactions:



Finally, in range IV, the model predicts a decrease in the concentration of metaborate units from the maximum value to zero. The proportion of $[\text{B}\text{O}_4]^-$ tetrahedra is reduced to zero, while the concentration of pyroborate $\text{B}\text{O}\text{O}_2^{2-}$ continues to grow. Hence it follows that reaction (5) is also valid for describing structural

transformations in the last (fourth) range. However, reaction (5) does not provide a complete idea of the modification of the local structure in the fourth range, since it does not give an idea of the decrease in the proportion of metaborate triangles against the background of the increase in the concentration of $\text{B}\text{O}\text{O}_2^{2-}$ units. Therefore, to describe the mechanisms of structural transformations in the last range, it is necessary to use an additional reaction involving metaborate triangles:



Consideration of the local distribution, whether only borate or only silicate (in this case, only borate), is not suitable for obtaining a visual representation of the modification of the local structure of glass with two network-forming cations. For these purposes, it is more convenient and clearer to use the total distribution of the structural units: in this case, the proportion of borate structural units calculated in relation to the total number of network-forming cations in the system. Having at our disposal the composition of the glass and the expressions describing the local distribution of borate units, it is quite easy to move from the local distribution to the general one. The dependences of the concentrations of borate structural units on the glass composition (n_4 ($[\text{B}\text{O}_4]^-$), n_{3s} (BO_3), n_{3a} ($\text{B}\text{O}_2\text{O}^-$), and n_{3p} ($\text{B}\text{O}\text{O}_2^{2-}$)), recalculated taking into account the total content of boron oxide in the $\text{Na}_2\text{O}-\text{B}_2\text{O}_3-$

SiO₂ system, are shown in Fig. 2. It can be seen that in the overall distribution, the maximum possible values of the concentrations of different types of basic borate groups gradually decrease with an increase in the value of parameter K . This is quite logical, since with the growth of K the content of boron oxide in the system decreases and, consequently, the actual total concentration of all possible borate units decreases.

Within the range of glass composition changes for which the Dell model was developed, we find that the maximum concentration of borate tetrahedra varies from 0.5, for binary sodium borate glass with a composition of 0.33Na₂O·0.67B₂O₃, up to 0.2 in borosilicate glass with $K = 8$. The maximum concentration of symmetrical triangles for the same limit values of K varies from 1 (glass-like B₂O₃) to 0.15. The proportion of metaborate triangles varies from 0.33 (binary glass) to 0 (in the context of $K = 8$ the model does not assume the existence of such structural units for any R) and, finally, the maximum concentration of pyroborate units will vary from 1, in binary sodium borate glass, to 20% in borosilicate glass with an extremely high value of K .

Obviously, knowledge of the distribution of only borate structural units in borosilicate glass does not give a complete picture of its structure. It is also necessary to know the distribution of silicate structural units. The Dell model, explicitly, that is, in the form in which it is presented in Table 1 does not provide such information. The exception is the first range, where, according to the model, the modification of silicate structural units is completely absent, which means that only completely polymerized Q⁴ units are present. Nevertheless, knowing the distribution of borate structural units, we can obtain the necessary information about the distribution of silicate structural units. For this, it is convenient to use the concept of the average charge of a structural unit. In the case of a system with monovalent modifier cations, this value will be numerically equal to the ratio of the number of modifying cations to the total number of network-forming cations:

$$\bar{q} = \frac{2[\text{Na}_2\text{O}]}{[\text{SiO}_2] + 2[\text{B}_2\text{O}_3]}, \quad (7)$$

or

$$\bar{q} = \frac{2R}{2 + K}, \quad (8)$$

if we substitute the oxide concentrations expressed in parameters R and K into Eq. (7):

$$[\text{Na}_2\text{O}] = \frac{R}{R + K + 1}, \quad (9)$$

$$[\text{B}_2\text{O}_3] = \frac{1}{R + K + 1}, \quad (10)$$

$$[\text{SiO}_2] = \frac{K}{R + K + 1}. \quad (11)$$

However, the average charge of a structural unit can be expressed in terms of the concentrations of structural units:

$$\begin{aligned} \bar{q} = & \frac{2}{2 + K}(N_4 + N_{3a} + 2N_p) \\ & + \frac{K}{2 + K}(N_{Q^3} + 2N_{Q^2} + 3N_{Q^1} + 4N_{Q^0}). \end{aligned} \quad (12)$$

In expression (12), N is the concentration of the corresponding type of borate or silicate units (the subscript indicates the type of structural unit) in the corresponding local distributions. Since the sum is known (determined by the composition of the glass, see Eq. (8)), the first term is also known, and it is not difficult to express the average charge of silicate structural units in terms of the concentrations of borate base groups and the glass composition (parameters R and K):

$$\begin{aligned} & N_{Q^3} + 2N_{Q^2} + 3N_{Q^1} + 4N_{Q^0} \\ = & \frac{2R}{K} - \frac{2}{K}(N_4 + N_{3a} + 2N_p). \end{aligned} \quad (13)$$

At the same time, the average charge of silicate structural units is known to be numerically equal to the average number of nonbridging oxygen atoms per silicon atom. In binary alkaline silicate systems, the average number of nonbridging oxygen atoms per silicon atom is as follows:

$$\frac{HMK}{\text{Si}} = \frac{2x}{1 - x}, \quad (14)$$

where x is the concentration of the modifier oxide, expressed in mole fractions. Equating the right parts of Eqs. (13) and (14) and solving the resulting equality with respect to x , we obtain that part of the modifying oxide that is spent on the modification of the silicate component of borosilicate glass:

$$x = \frac{R - (N_4 + N_{3a} + 2N_p)}{K + R - (N_4 + N_{3a} + 2N_p)}. \quad (15)$$

The results of calculations of the proportion of modifier oxide interacting only with silicate structural units are shown in Fig. 3. It can be seen that in any section with the given value of K , the maximum concentration of alkaline oxide consumed for the modification of the silicate subnetwork is 50%; i.e., the local Qⁿ distribution changes from $N_{Q^4} = 1$ (it corresponds to the first range of the Dell model, where there is no modification of silicate structural units) up to a distribution corresponding to glass of the metasilicate composition (0.5Na₂O·0.5SiO₂).

The concentrations of silicate structural units in the local representation can be obtained in different ways. It is possible to calculate the local distribution for the binary sodium silicate system using the k_3 and k_2 of the disproportionation reactions,

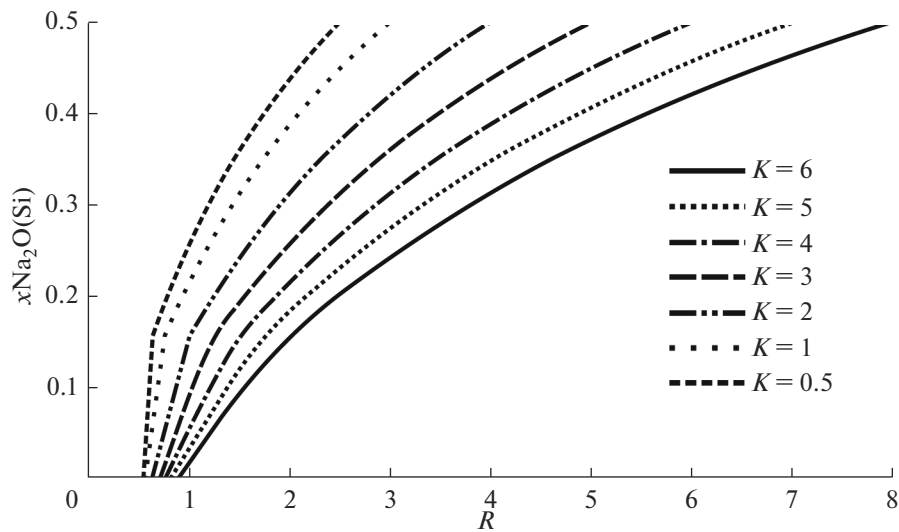
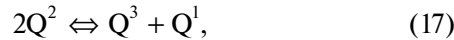


Fig. 3. The proportion of alkaline oxide spent on the modification of the silicate component of the disordered network of borosilicate glass for sections with $K = 0.5, 1, 2, 3, 4, 5,$ and 6 .



which determine the equilibrium concentrations in binary sodium silicate glasses whose composition varies from pure SiO_2 ($x = 0$) to sodium metasilicate ($x = 0.5$) by solving the following system of equations:

$$\left\{ \begin{array}{l} N_{Q^4} + N_{Q^3} + N_{Q^2} + N_{Q^1} = 1 \\ N_{Q^3} + 2N_{Q^2} + 3N_{Q^1} = \frac{2x}{1-x} \\ k_3 = \frac{N_{Q^4}N_{Q^2}}{N_{Q^3}^2} \\ k_2 = \frac{N_{Q^3}N_{Q^1}}{N_{Q^2}^2} \end{array} \right. \quad (18)$$

For example, according to the data ^{29}Si NMR [5], $k_3 = 0.02$ ($2Q^3 \Leftrightarrow Q^4 + Q^2$) and $k_2 = 0.06$ ($2Q^2 \Leftrightarrow Q^3 + Q^1$) for glasses of the sodium silicate system at room temperature. However, in this study, we used a different approach: we used the previously developed three-parameter statistical algorithm for modeling Q^n distributions in binary alkaline silicate systems [6, 7]. As can be seen from Fig. 4, this approach provides a fairly reasonable description of the experimental data available in the literature [5, 8–13] (shown in the figure by symbols) on the local structure of glasses of the Na_2O – SiO_2 system in the range of interest.

The transition from the local Q^n distribution characteristic of the binary Na_2O – SiO_2 system, to the total distribution (in terms of the total number of silicate and borate structural units in borosilicate glass) gives the following picture (Fig. 5) of changes in the con-

centration of different types of silicate structural units in the glasses under consideration. As can be seen from Fig. 5, with the growth of K , the maximum concentrations of Q^n units grow, which is quite logical, since the concentration of silicon oxide increases and, consequently, the number of silicate structural units increases. Of the four Q^n units that can be formed in the system ($n = 4, 3, 2,$ and 1), only Q^3 units demonstrate the nonmonotonic nature of the change, while the concentration of Q^4 units systematically decreases, and the concentrations of Q^2 and Q^1 units systematically increase with increasing R within each section with a constant value of parameter K . This is also logical, since in the previously shown binary distribution, only the concentration of Q^3 units changed nonmonotonically in the range of compositions in which the Dell model works. Moreover, it can be noted that the value R , at which the concentration of the Q^3 units reaches its maximum, depends on the content of SiO_2 in glass and systematically shifts to the region of large values with a gradual increase in the value of K .

Combining the data on the concentrations of borate and silicate structural units (Figs. 2, 5), we can get a complete picture of the distribution of basic structural units in sodium borosilicate glasses. As an example, two distributions are shown for sections with $K = 0.5$ and 2 in Fig. 6. These distributions give a fairly complete idea of the predictions of the Dell model in terms of changes in the local structure of glass within each selected section with a constant value of parameter K and also allow us to see the general patterns of changes in the structure of glasses when this parameter is changed. However, the question of what can be learned from the Dell model regarding the presence or absence of borate or mixed borosilicate superstruc-

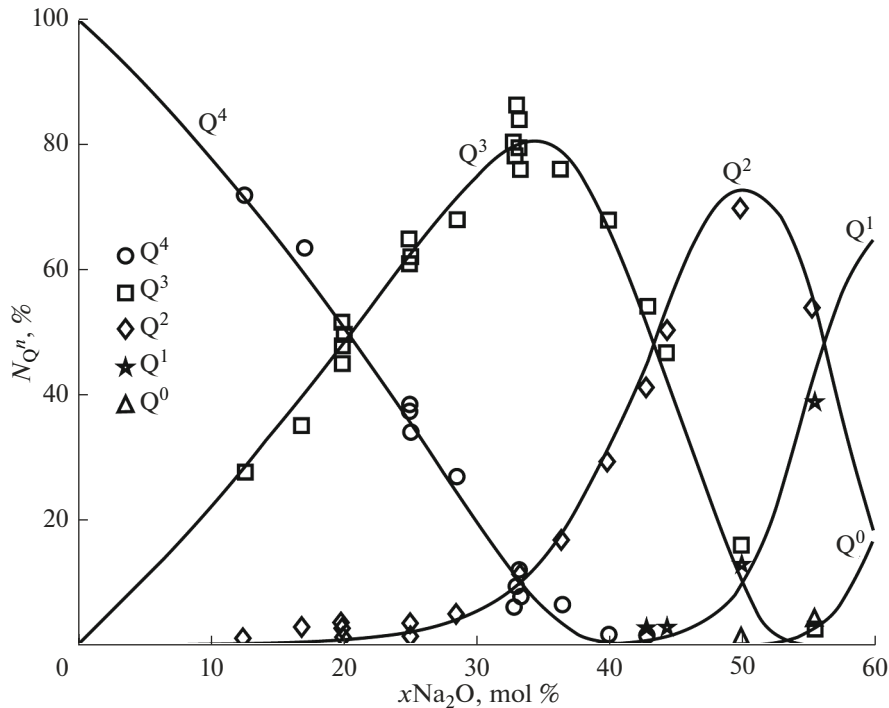


Fig. 4. Simulation results (lines) of Q^n distribution in glasses of the $\text{Na}_2\text{O}-\text{SiO}_2$ system. Symbols are experimental data [5, 8–13].

tural groups in the structure of borosilicate glass of various types remains open.

As follows from Table 1, the model does not explicitly address this issue. From the most general considerations, it can be assumed that since mixed borosilicate rings (danburite or reedmergnerite) consist of borate tetrahedra and Q^4 units, these rings will be formed in the region of compositions where the Q^4 units and borate tetrahedra are present simultaneously in the maximum number, i.e., where the product of the concentration of these structural units has a maximum. The dependence of the change in the product of concentrations Q^4 and $[\text{BO}_4]^-$ units of the glass composition for a number of selected sections with a constant value of K is shown in Fig. 7a. It can be seen that this product strongly depends on the ratio of glass-forming oxides in the system: as the value of K increases from 0.5, the maximum value of the product increases rapidly and, in the section of $K = 4$, becomes maximum and then slightly decreases (see Fig. 7b). Within each specific section with a fixed value of K , with the growth of R , the value of the product $n_{Q^4} \cdot n_4$ increases quite rapidly and, after reaching the maximal value, gradually begins to decrease. It can also be noted that the range of values R , within which the product $n_{Q^4} \cdot n_4$ reaches its maximum is quite narrow: $0.525 \leq R \leq 0.875$ when K varies from 0.5 to 6. The position of the points corresponding to the maximum values of the product of the concentrations of fully polymerized borate and silicate tetrahedra is shown in

the triple composition diagram. All of them visually fit on one straight line. According to the assumption made earlier, it can be expected that glasses whose compositions lie near this straight line will be characterized by an increased (relative to glasses of other compositions) content of mixed borosilicate rings.

It obviously does not make much sense to compare the predictions of the Dell model regarding the change in the concentration of borate structural units as a function of the glass composition, since these data underlie the model, which is effectively a piecewise linear approximation of the corresponding experimental dependences. It is much more interesting to evaluate the correctness of the model's predictions regarding the modification of the silicate component of the disordered network of sodium borosilicate glasses. This point will be considered in the next section.

THERMODYNAMIC MODEL

The next model considered in this paper is the thermodynamic (TD) model developed by the staff of the Grebenshchikov Institute of Silicate Chemistry, Russian Academy of Sciences. It can be immediately noted that, unlike the Dell model, which is based on a set of experimental data on the structure of sodium borosilicate glasses accumulated by the time of its creation, the TD model does not rely on empirical structural information when modeling the glass structure.

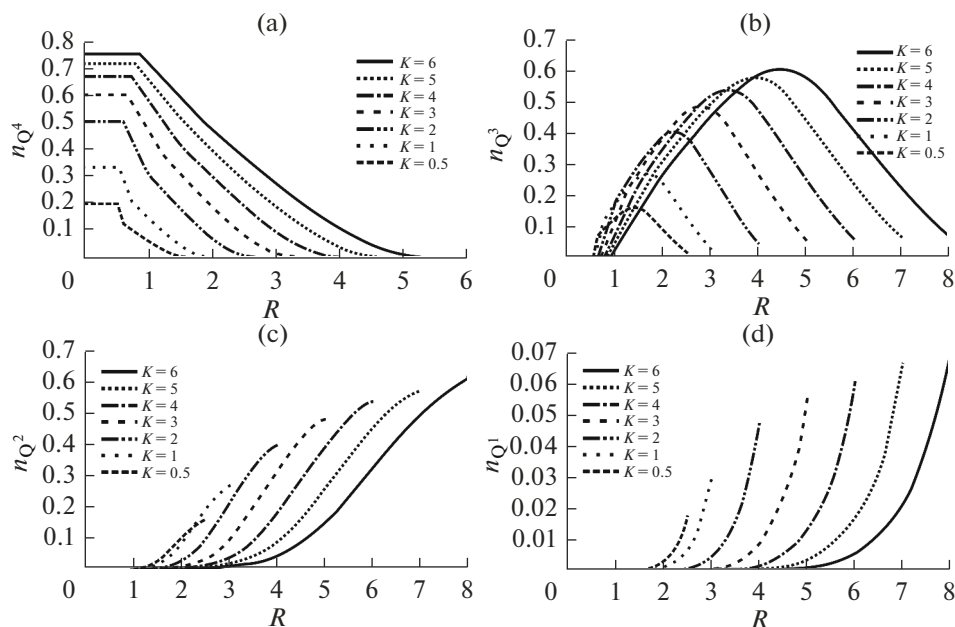


Fig. 5. Q^n concentrations of units in sodium borosilicate glasses of sections with $K = 0.5, 1, 2, 3, 4, 5,$ and 6 as a function of parameter R , calculated relative to the total amount of network-forming cations in the system.

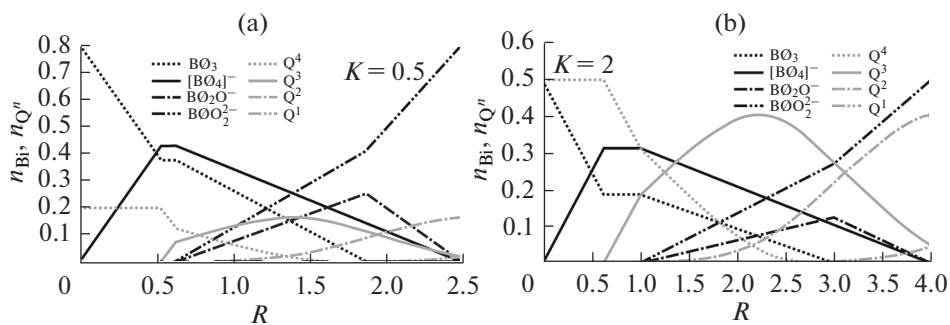


Fig. 6. Examples of the distribution of basic structural units in sodium borosilicate glasses—the Dell model.

Without completing the exposition of the TD approach to modeling the structure and properties of glass-like materials, we will briefly outline its fundamental ideas. (More detailed information about the principles of the TD approach to modeling the structure and properties of oxide glasses and glass-forming melts can be found, for example, in [14, 15]). In this approach, glasses and melts are considered as solutions of chemical groups, which are salt-like products of the reactions of the interaction of the initial oxides and unreacted oxides. In their stoichiometry, salt-like products coincide with crystalline compounds that exist in the phase diagram of the studied system and, therefore, the choice of chemical groups for each specific system is based on the analysis of the corresponding phase diagrams. In particular, for the $\text{Na}_2\text{O}-\text{B}_2\text{O}_3-\text{SiO}_2$ system, this analysis yields two ternary compounds ($\text{Na}_2\text{O}\cdot\text{B}_2\text{O}_3\cdot 2\text{SiO}_2$, $\text{Na}_2\text{O}\cdot\text{B}_2\text{O}_3\cdot 6\text{SiO}_2$),

eight binary borates ($\text{Na}_2\text{O}\cdot 9\text{B}_2\text{O}_3$, $\text{Na}_2\text{O}\cdot 5\text{B}_2\text{O}_3$, $\text{Na}_2\text{O}\cdot 4\text{B}_2\text{O}_3$, $\text{Na}_2\text{O}\cdot 3\text{B}_2\text{O}_3$, $\text{Na}_2\text{O}\cdot 2\text{B}_2\text{O}_3$, $\text{Na}_2\text{O}\cdot \text{B}_2\text{O}_3$, $2\text{Na}_2\text{O}\cdot \text{B}_2\text{O}_3$, $3\text{Na}_2\text{O}\cdot \text{B}_2\text{O}_3$), five binary silicates ($3\text{Na}_2\text{O}\cdot 8\text{SiO}_2$, $\text{Na}_2\text{O}\cdot 2\text{SiO}_2$, $\text{Na}_2\text{O}\cdot \text{SiO}_2$, $3\text{Na}_2\text{O}\cdot 2\text{SiO}_2$, $2\text{Na}_2\text{O}\cdot \text{SiO}_2$), and three initial oxides (Na_2O , B_2O_3 , SiO_2) [15–17]. Each of the reactions of the formation of ternary and binary compounds is characterized by its standard Gibbs free energy, and the equilibrium amounts of chemical groups is determined by minimizing the free energy of the system as a whole. The latter is achieved by solving the system of mass balance equations for the components and the law of mass action for all reactions occurring in a system of the given composition [14]. Solving such a system results in information about the equilibrium amounts of chemical groups as a function of glass composition, which is called the chemical structure of glass. Exam-

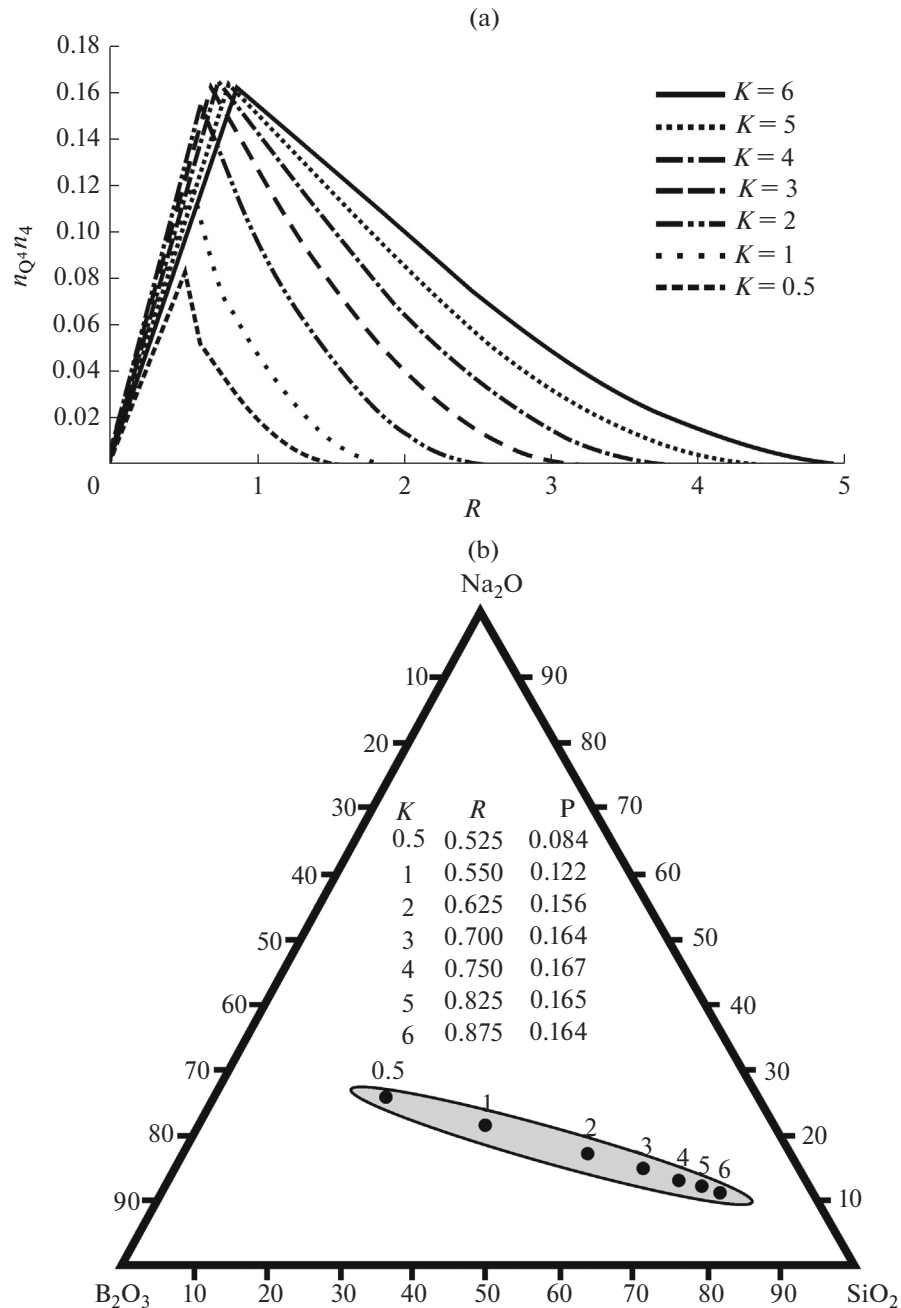


Fig. 7. The product of the concentrations of fully polymerized silicate (Q^4) and borate ($[B\emptyset_4]^-$) units in sodium borosilicate glasses (a) and the range of compositions where the presence of mixed borosilicate (danburite or reedmergnerite) rings are most likely to be present in the glass structure (b). (Column P contains the numerical values of the product $n_{Q^4} \cdot n_4$).

ples of these equations for sodium borosilicate glasses can be found in [15–17]. The transition from the chemical structure of glass to the distribution of basic structural units or superstructural groups is carried out within the framework of the assumption and structural similarity of chemical groups and crystals corresponding to them in terms of the stoichiometry of the ratio of different basic structural units or superstructural groups. Thus, if we know the number of chemical

groups in a system of the given composition and have information about the structure of the corresponding crystalline compounds at the level of basic structural units or superstructural groups (the latter is relevant for boron-containing glasses), we can obtain the desired distributions.

Figure 8a presents the results of the TD modeling of the structure of soda borosilicate glasses concerning the concentration of borate tetrahedra as a function of

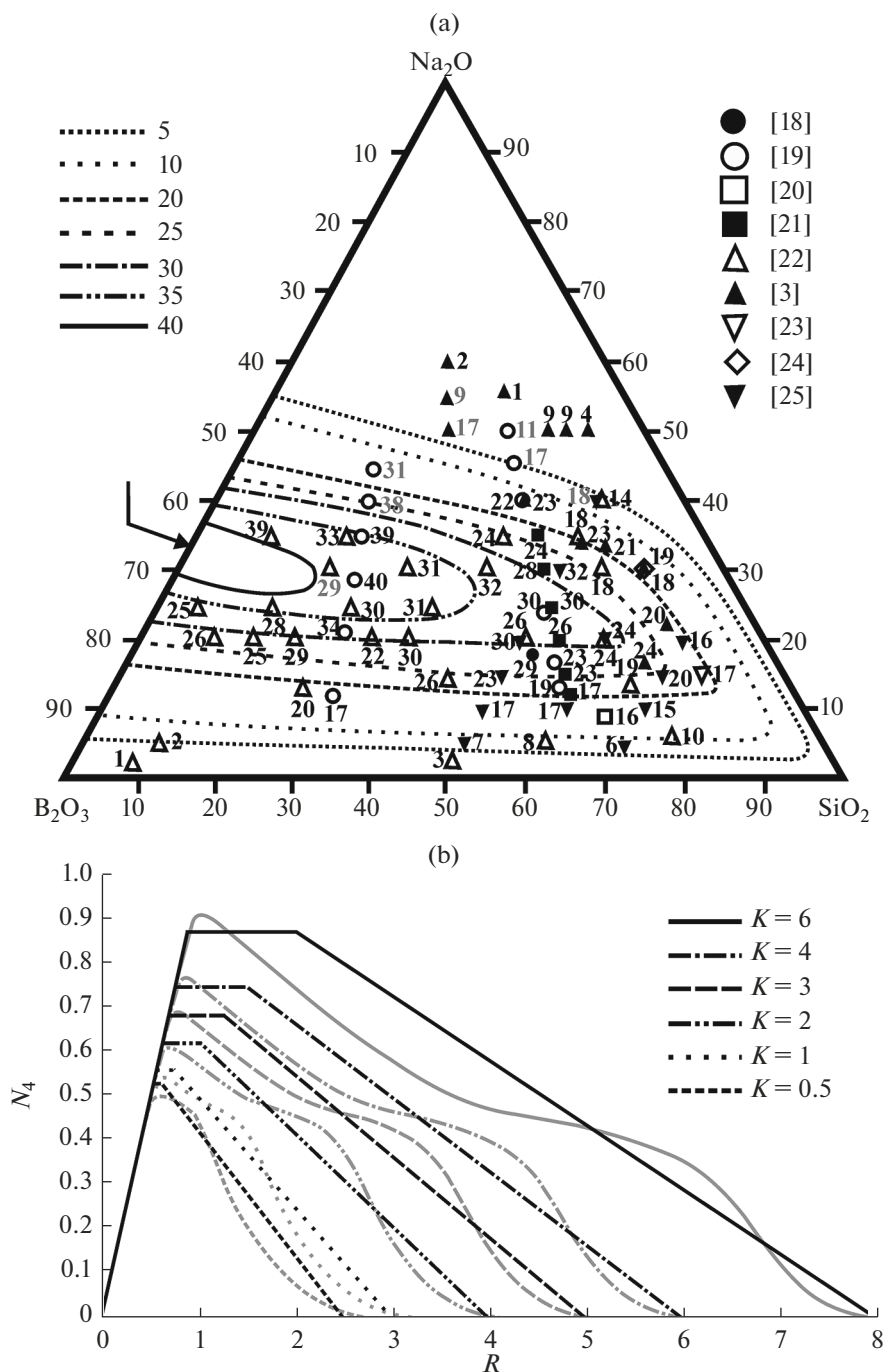


Fig. 8. The concentration of tetrahedra $[\text{BO}_4]^-$ in sodium borosilicate glasses. Comparison of the results of TD modeling (isoconcentration lines) with the experimental data (symbols, numbers near the symbols correspond to the concentrations of borate tetrahedra in glass of the given composition) (a), comparison of TD simulation results (smooth gray lines) with the Dell model (black broken lines) (b). The values calculated in relation to the total amount of network-forming cations in the system are given in (a). The curves in (b) represent the change in the concentration of borate tetrahedra in the local representation (the proportion of tetrahedra $[\text{BO}_4]^-$ in relation to the total number of borate structural units).

glass composition. This figure is a reconstruction of Fig. 9 published in [17] (the calculation results are presented in the form of isoconcentration lines) on which the corresponding experimental data [3, 18–25] obtained by various authors were additionally plotted.

(All subsequent figures showing the results of the TD modeling of the structure of sodium borosilicate glasses are also reconstructions of the corresponding figures from [17], on which additional information was applied). It follows from the figure that in glasses of

the $\text{Na}_2\text{O}-\text{B}_2\text{O}_3-\text{SiO}_2$ system, the concentration of borate tetrahedra cannot exceed 43%: this value corresponds to the content of the $[\text{B}\text{O}_4]^-$ units in a binary glass of the $0.33\text{Na}_2\text{O}\cdot 0.67\text{B}_2\text{O}_3$ composition (indicated by an arrow in the figure). Tracking the values of the concentrations of borate tetrahedra in glasses of various compositions shown in the figure along (near) the isoconcentration curves, it is easy to see that the bulk of the experimental data agrees quite well with the predictions of the TD model both at the qualitative and quantitative levels. For example, near the isoconcentration line, for which $n_4 = 20\%$, the concentrated experimental data values lie approximately in the interval of 16 to 26%, and the scatter of experimentally determined concentrations of borate tetrahedra in glasses whose compositions are located near the curve with $n_4 = 30\%$ is 22–34%. In general, out of the 74 experimentally determined values shown in the figure, the discrepancy between the model and experiment appears quite significant only for 8 glasses (these values are highlighted in gray in the figure). These “unsatisfactory” values include the following values: $n_4 = 38\%$ { $\sim 25\%$ } ($0.2\text{SiO}_2\cdot 0.4\text{B}_2\text{O}_3\cdot 0.4\text{Na}_2\text{O}$) [19], 31% { $10\% \leq n_4 \leq 20\%$ } ($0.185\text{SiO}_2\cdot 0.371\text{B}_2\text{O}_3\cdot 0.444\text{Na}_2\text{O}$) [19], 29% ($0.2\text{SiO}_2\cdot 0.5\text{B}_2\text{O}_3\cdot 0.3\text{Na}_2\text{O}$) { $35\% \leq n_4 \leq 40\%$ } [22], 9% ($0.222\text{SiO}_2\cdot 0.222\text{B}_2\text{O}_3\cdot 0.556\text{Na}_2\text{O}$) { $n_4 \leq 5\%$ } [3], 17% ($0.25\text{SiO}_2\cdot 0.25\text{B}_2\text{O}_3\cdot 0.5\text{Na}_2\text{O}$) { $n_4 \leq 5\%$ } [3], 11% ($0.333\text{SiO}_2\cdot 0.167\text{B}_2\text{O}_3\cdot 0.5\text{Na}_2\text{O}$) { $n_4 \leq 5\%$ } [19], 17% ($0.364\text{SiO}_2\cdot 0.182\text{B}_2\text{O}_3\cdot 0.455\text{Na}_2\text{O}$) { $\sim 5\%$ } [19], and 18% { $5\% \leq n_4 \leq 10\%$ } ($0.5\text{SiO}_2\cdot 0.1\text{B}_2\text{O}_3\cdot 0.4\text{Na}_2\text{O}$) [25]. (The values in curly brackets correspond to the predictions of the TD model).

Figure 8b compares the predictions of the Dell model (black broken lines) and the TD model (gray smooth curves) regarding the change in the concentration of borate tetrahedra in the structure of glasses of the $\text{Na}_2\text{O}-\text{B}_2\text{O}_3-\text{SiO}_2$ system in sections with $K = 0.5, 1, 2, 3, 4,$ and 6 (the TD simulation data are a reconstruction of Fig. 3 from [16]). The presented dependences characterize the proportion of borate tetrahedra with respect to borate structural units only (local representation). It can be seen that both models, in general, do not contradict each other. Moreover, in range I according to Dell (see Table 1) both models give identical results for all the presented sections. However, for large values of R this quantitative identity deteriorates somewhat. The TD model does not assume the existence of dependence N_4 on the glass composition of the area where the concentration of tetrahedra $[\text{B}\text{O}_4]^-$ remains unchanged (section II in the Dell model), of a simple linear change in the concentration of the 4-coordinated boron atoms in ranges III and IV (according to Dell) or any kinks characteristic of the Dell model (transitions from range I to II and II to III). Since the Dell model is, in essence, a piecewise linear approximation of the experimental data, the selection of certain ranges in it with clear

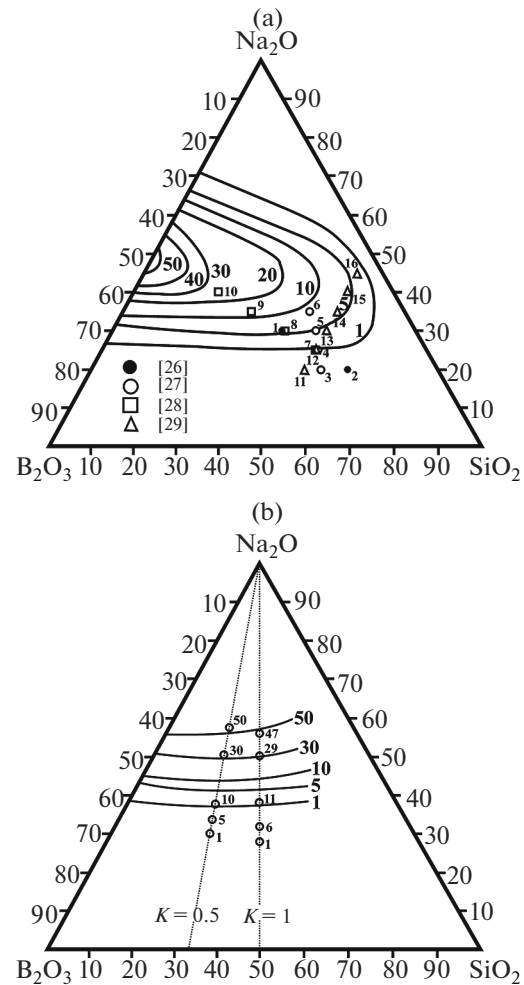


Fig. 9. Concentrations of metaborate (a) and pyroborate (b) groups in glasses of the $\text{Na}_2\text{O}-\text{B}_2\text{O}_3-\text{SiO}_2$ system. The solid lines are the results of TD modeling (the large numbers near the solid lines are the numerical values of the concentrations of metaborate and pyroborate units in glasses whose compositions lie on the given isoconcentration line), small numbers near the symbols in (a) denote the ordinal numbers of the glasses studied in [26–29]. Small numbers for the symbols in (b) are the concentrations of pyroborate units calculated in the Dell model for glasses from two sections with $K = 0.5$ and 1 .

boundaries is mathematically justified, but an artificial separation. The TD model does not resort to any similar artificial simplifications and any changes in the dependence curves N_4 on the composition is a direct consequence of the change in the chemical structure of the glass, which, in turn, is the result of solving one single system of equations for the mass balance of the components and the law of mass action for all reactions occurring in the system.

It is shown in Figs. 9a and 9b the how the concentration of metaborate (asymmetric triangles $\text{B}\text{O}_2\text{O}^-$ and ring $\text{B}_3\text{O}_6^{3-}$ anions) and pyroborates ($\text{B}\text{O}\text{O}_2^{2-}$) of atomic groups in glasses of the $\text{Na}_2\text{O}-\text{B}_2\text{O}_3-\text{SiO}_2$ sys-

tem changes depending on their composition in the form of isoconcentration lines. Unfortunately, the literature almost completely lacks quantitative information on the concentration of various types of trigonal borate units with nonbridging oxygen atoms. In such a situation, only a qualitative comparison of theoretical calculations with the experiment is possible (but not always). It is known that vibrations of the terminal oxygen atoms of asymmetric metaborate triangles produce in the Raman spectra a band with the maximum in the region of 1410 to 1490 cm^{-1} . Therefore, by changing the intensity of this band, we can assess the changes in the concentration of this type of borate units. The numbered symbols in Fig. 9a correspond to the compositions of sodium borosilicate glasses, whose spectra were published in various works [26–29]. As follows from the spectra published in [26], in the spectrum of glass with the serial number 2, the intensity of the scattered signal in the region 1410–1490 cm^{-1} is extremely small, while in glass with number 1 it is much higher. Such a change in the intensity of the 1410–1490 cm^{-1} is entirely consistent with the predictions of the TD model. Indeed, point 2 lies outside the isoconcentration line with the minimum calculated value of the concentration of metaborate structures (1%), while point 1 is near the line describing the compositions of those glasses in which the concentration of metaborate groups is 5%. The Raman spectra of glasses whose compositions are numbered in Figs. 9a from 3 to 6 were published in [27]. The authors of this study showed that as the glass composition changes in the direction from point 3 to point 6, there is a systematic increase in the intensity of the band with the maximum near 1480 cm^{-1} (see Fig. 2c [27]). Based on the structural origin of this line, the behavior of its intensity indicates an increase in the concentration of metaborate groups with the indicated change in the glass composition. It is this situation that is predicted by the TD model. The strongest changes in the scattering intensity in the region 1410–1490 cm^{-1} are observed in the spectra presented in [28] (see Fig. 2 [28]). The compositions of the glasses studied in [28] are numbers 7–10 shown in Fig. 9a, while the increase in the intensity of the Raman signal in the indicated range of wave numbers occurs in the direction from glass with serial number 7 to glass 10. According to the results of TD modeling, the change in the glass composition in this direction should be accompanied by a significant increase in the concentration of metaborate groups: from $\sim 1\%$ to a value lying in the range of 20 to 30%, which fully corresponds to the nature of the change in the high-frequency band in the Raman spectra presented in [28]. Finally, it was very interesting and useful to compare the model results with the features of the Raman spectra of glasses whose compositions form the section shown in Fig. 9a with triangles numbered 11 to 16. According to the TD modeling data, in this section, in the direction from point 11 to point 16, the concentra-

tion of metaborate groups should change nonmonotonically. In other words, when the glass composition changes from point 11 to point 13, the concentration of metaborate groups gradually increases. Then it can be seen that points 13, 14, and 15 lie near the same 5% isoconcentration line; i.e., there are no significant changes in the content of the considered borate groups, and further on (point 16), their concentration will decrease. This behavior of the intensity of the 1410–1490 cm^{-1} line can be detected by analyzing the spectra presented in Fig. 2a in [29]. Thus, although these examples are not a rigorous proof of the correctness of the prediction of the TD model regarding the behavior of metaborate groups, they clearly testify in its favor.

As for pyroborate $\text{B}\ddot{\text{O}}\text{O}_2^{2-}$ units, according to the data of TD modeling (Fig. 9b), their concentration within each section with a constant value $K < 2$ is a monotonically increasing function of the ratio of sodium oxide to the boron oxide content in glass (parameter R). Comparison of the data of the TD model with the experiment in this case is impossible even at a qualitative level, since the information required for such a comparison is not available in the published data. Therefore, here we limited ourselves to comparing the predictions of two models: the Dell model and the TD model. The results of calculating the concentration of $\text{B}\ddot{\text{O}}\text{O}_2^{2-}$ units for several compositions from sections with $K = 0.5$ and 1 are shown as symbols in the figure. The numbers next to the symbols correspond to the calculated concentrations. It can be seen that with full qualitative agreement between the predictions of both models, the Dell model suggests that the formation of pyroborate units in the glasses under consideration begins at slightly lower values of ratio R than it follows from the results of TD simulation. As a consequence, for glasses whose compositions lie near the isoconcentration line with a 1% content of $\text{B}\ddot{\text{O}}\text{O}_2^{2-}$ triangles, Dell's model gives almost 10 times higher concentrations. However, as R increases the quantitative discrepancy between the model data decreases and both models give almost identical values for those glasses where the expected content of pyroborate units according to TD modeling is 30% or more.

Let us now turn to silicate structural units, paying attention, for example, to the concentrations Q^3 (Fig. 10a) and Q^2 (Fig. 10b) units in glasses of the considered system. As can be seen from Fig. 10a, the TD model predicts a nonmonotonic character of the change in concentration of Q^3 units (the presence of a maximum on the dependence $n_4(R)$ for a fixed K) when the glass composition changes along the sections with a constant ratio of network-forming oxides. For example, the figure shows four sections with $K = 0.5, 2, 4,$ and 6. This behavior of the content of silicate tetrahedra with one nonbridging oxygen atom is in com-

plete agreement with the experimentally established trends in the change in the concentration of these structural units with the corresponding change in the glass composition. Moreover, based on Fig. 10a, we can see good quantitative agreement between the theoretical calculations and experimental data. This concerns both the determination of the compositions of glasses with the maximum concentration of Q^3 units and the actual content of this type of silicate tetrahedra in glasses. With regard to the last statement, however, it should be noted that the TD model often gives slightly higher concentrations of Q^3 units compared to the experimentally determined values (Fig. 10a).

As for the Q^2 units (Fig. 10b), there is a very good, both qualitative and quantitative, agreement between the theoretical calculations and the experiment. For example, as can be seen from Fig. 10b, in glasses whose compositions are located near the isoconcentration line with $n_{Q^2} = 1\%$, the experimentally determined concentrations lie in the range 0–6%, while along the line with $n_{Q^2} = 40\%$, the concentration of Q^2 units according to different authors ranges from 36 to 47%. On the whole, both the theory and experiment show that in glasses with a constant value of parameter K the fraction of silicate tetrahedra with two nonbridging oxygen atoms systematically increases with an increase in ratio R .

Performing a similar comparison of the experimental data on the concentration of Q^3 units with the predictions of the Dell model (Fig. 11), it can be seen that this model gives the maximum possible concentrations of the Q^3 units in the corresponding sections ($K = 0.5, 2, 4,$ and 6). However, in this case, the compositions of glasses, where such a maximum is reached, are quite different from those for which the maximum values were found experimentally. This difference is most pronounced in the glasses of sections with small values of the parameter K and, to a lesser extent, is characteristic of glasses of sections with higher values of the ratio of silicon oxide to boron oxide.

As follows from Fig. 12, Dell's model correctly predicts the increase in Q^2 units with the increasing parameter value R , but the experimental data testify in favor of the fact that such units begin to form in sodium borosilicate glasses somewhat earlier (at lower values of R) than is assumed by the model. As in the case of Q^3 units, the quantitative agreement between the model and experiment improves when moving from sections with small values of ratio K to sections with higher values of this parameter.

It can be assumed that the delay in the formation of silicate structural units with nonbridging oxygen atoms in the glass structure (Figs. 11, 12) found in the model's predictions is a consequence of the fact that changes in the local structure of the borate and silicate components of the borosilicate glass network are con-

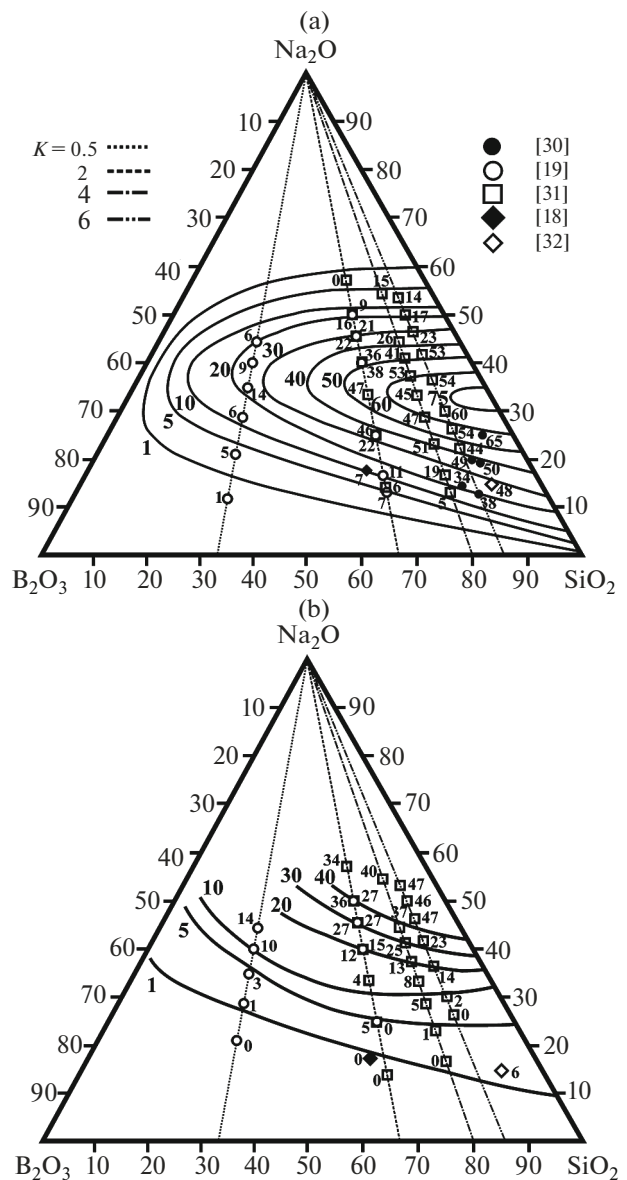


Fig. 10. Comparison of the results of the TD model with the experiment for the dependences of Q^3 (a) and Q^2 (b) units of glass composition in $\text{Na}_2\text{O}-\text{B}_2\text{O}_3-\text{SiO}_2$ system. Theoretical calculations are presented as isoconcentration lines (large numbers near the lines correspond to the concentration of the given type of silicate tetrahedra in glass). Symbols denote compositions of experimentally studied glasses. Small numbers near the symbols are experimentally determined concentrations of structural units.

sidered for each of them separately. As a result, a glass network modification mechanism such as the breaking of a mixed B–O–Si bridge bond is excluded from consideration, as a result of which borate and silicate structural units with terminal oxygen atoms can simultaneously form in the structure.

Let us return to consideration of the TD model. Unlike the Dell model, the predictive part of which is limited mainly by the local structure of the glass, the

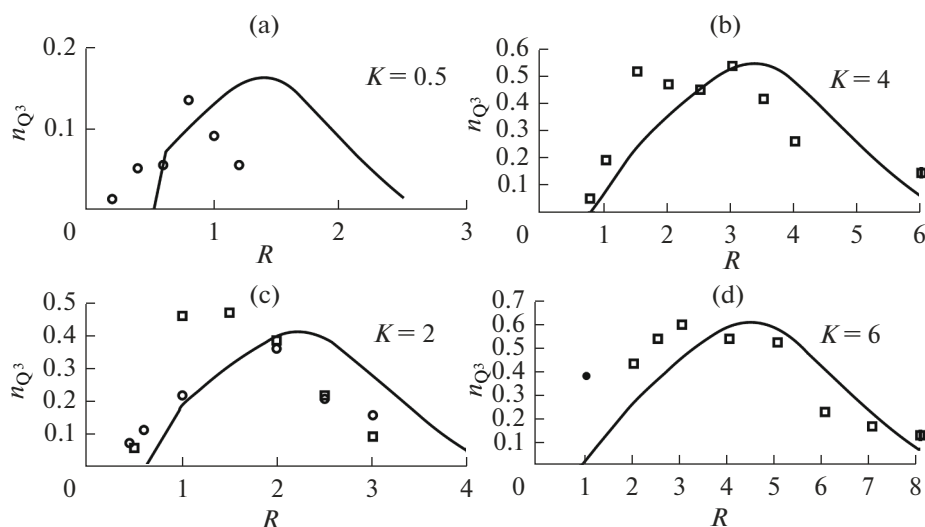


Fig. 11. Comparison of predictions of the Dell model on the concentration of Q^3 units in sodium borosilicate glasses of sections with $K = 0.5, 2, 4,$ and 6 (lines) with experimental data (symbols: circles, [19], squares, [31], black circle, [30]).

TD model provides information not only on the distribution of basic structural units in glass but also allows us to consider the issue of changing the glass structure on scales of the average order to obtain the dependence of the concentration of superstructural groups from the composition of the glass. Such data were published in [17] in the form of isoconcentration lines for boroxol rings; penta-, di-, and triborate groups (Fig. 2, [17]); and for mixed borosilicate danburite and reedmergnerite rings (Fig. 8, [17]). However, due to the fact that currently there are no experimental methods and techniques for the quantitative determination of the concentration of superstructural groups in boron-containing glasses, it is very difficult to assess the correctness of the TD model's predictions for these structures. Proceeding from this, in this paper we will restrict ourselves to a qualitative analysis of the correspondence between the theoretical calculations and the experiment using the example of boroxol rings. The presence of such groups in glass is unambiguously identified by Raman spectroscopy along the narrow line with the maximum near 808 cm^{-1} , which allows the necessary analysis to be carried out.

The content of boroxol rings in sodium borosilicate glasses of various compositions is shown in Fig. 13, where the symbols denote the compositions of those glasses whose Raman spectra were published in [29] (circles) and [27] (diamonds). Glass compositions with numbers ranging from 1 to 7 correspond to the section with $x_{\text{SiO}_2} = 50\text{ mol } \%$. According to the spectra published in [29], the intensity of the 808 cm^{-1} is high in the glass spectrum at number 1. As the glass composition changes in the direction from 1 to 4, the intensity of this line rapidly decreases, and this line is no longer observed in the spectra of glasses with numbers above 4 (Fig. 2a, [29]). A similar situation is typ-

ical for the spectra of glasses in the section with $x_{\text{SiO}_2} = 67\text{ mol } \%$ (numbers 8–14). Line 808 cm^{-1} has the highest intensity in the spectra of this section in the spectrum of glass number 8. However, here it is much smaller than in the spectrum of glass number 1. When the glass composition changes in the direction from 8 to 12, the intensity of the characteristic vibration band of boroxol rings decreases; however, this occurs much more slowly than in the spectra of the glasses of the previous section, and in the spectra of the last two glasses (13, 14), this line is completely absent (Fig. 2b, [29]). Further, the analysis of the Raman spectroscopy data for the glasses of the section with $K = 2.12$ (diamonds in Fig. 13) allowed the authors of [27] to establish that when the glass composition changes in the direction from composition 15 to 20, the integrated intensity (area) of line 808 cm^{-1} systematically decreases almost to zero (Fig. 2a, [27]). It is easy to see from Fig. 13 that all the described changes in the intensity of the 808 cm^{-1} are in good agreement with the predictions of the TD model.

To conclude this section, let us turn to the predictions of the TD model regarding the content of $\text{Na}_2\text{O}-\text{B}_2\text{O}_3-\text{SiO}_2$ mixed borosilicate danburite and reedmergnerite rings. Such data are shown in Fig. 14. Additionally, in this figure, the region of compositions is highlighted in gray, where, according to the Dell model, the product of the concentrations of borate tetrahedra and Q^4 units has the maximum value. Recall that the formation of mixed borosilicate rings in glasses is most likely to be expected in this region. Thus, it can be seen that the estimation of the composition of glasses characterized by an increased content of borosilicate rings based on the data on the concentration of basic structural units (according to the Dell

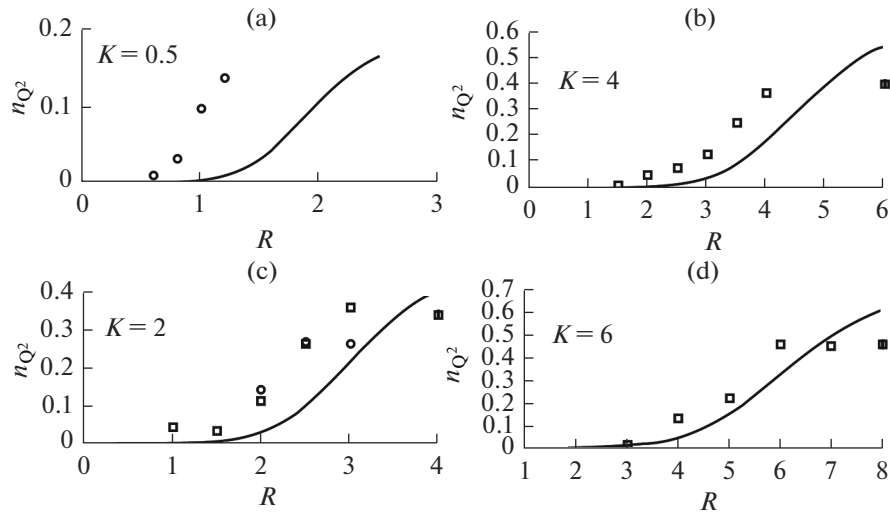


Fig. 12. Comparison of the Dell model's predictions regarding the change in concentration of Q^2 units in sodium borosilicate glasses of sections with $K = 0.5, 2, 4,$ and 6 (lines) with experimental data (symbols: circles, [19]; squares, [31]).

model) and the results of the corresponding calculations within the TD approach are in good agreement with each other.

The dashed lines in Fig. 14 indicate the six sections: three with a constant ratio R and three with a constant

ratio K . The points of intersection of these lines correspond to the glass compositions that were investigated by Du and Stebbins [33] for the nearest environment of borate structural units in sodium borosilicate glasses. Of all the configurations of the local environ-

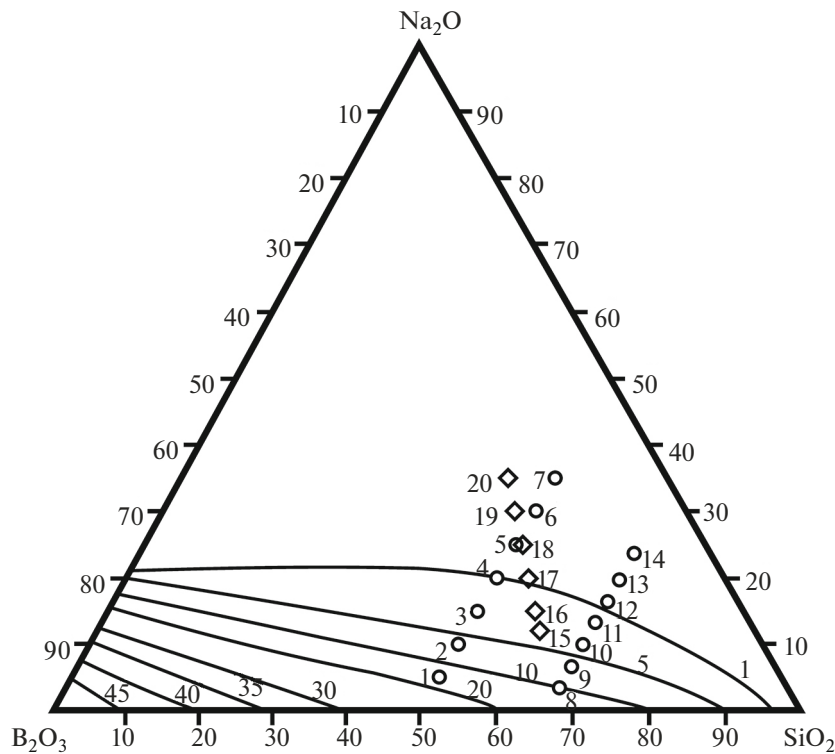


Fig. 13. The content of boroxol B_3O_3 rings in glasses of the Na_2O - B_2O_3 - SiO_2 system. The solid lines are the results of TD modeling (large numbers near the solid lines are the numerical values of the concentrations of boroxol rings in glasses whose compositions lie on the given isoconcentration line), the symbols are the compositions of the glasses studied in [29] (circles) and [27] (diamonds). The numbers next to the symbols are serial numbering.

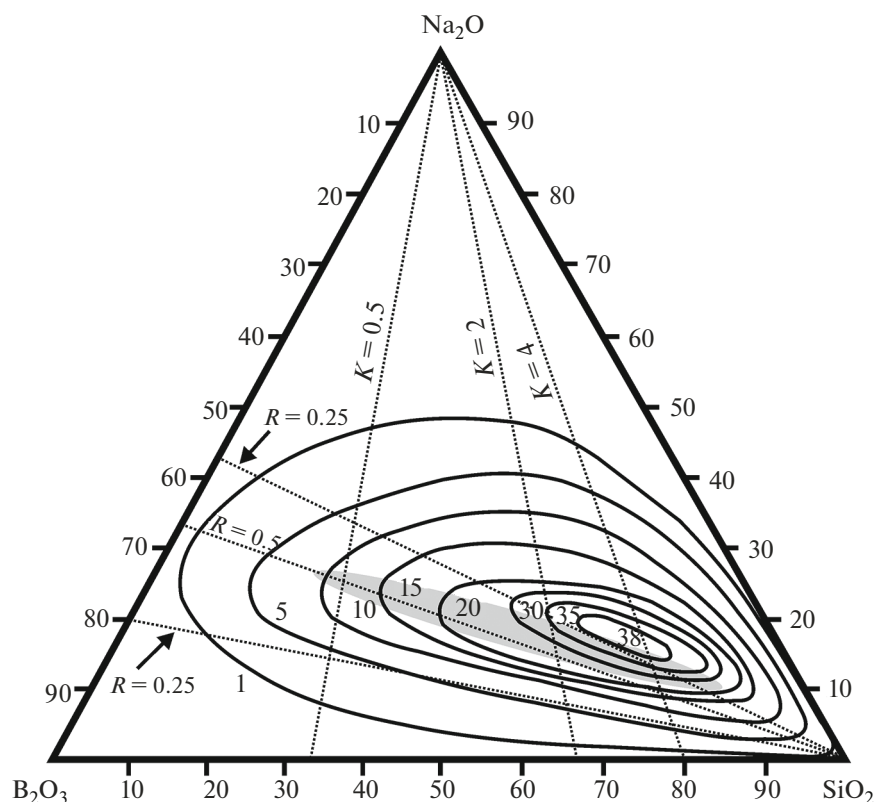


Fig. 14. The total content of mixed borosilicate danburite and reedmergnerite rings in glasses of the $\text{Na}_2\text{O}-\text{B}_2\text{O}_3-\text{SiO}_2$ system according to TD modeling data. The numbers near the solid lines are the numerical values of the total concentration of danburite and reedmergnerite rings in glasses whose compositions lie on the given isoconcentration line. The region of glass compositions characterized by high values of the product $n_{\text{Q}^4} \cdot n_4$ (according to Dell) is highlighted in gray. Dashed lines are sections with constant ratios of parameters R and K .

ment of the basic borate structural units studied by these authors, two configurations are of interest in this context: $^{14}\text{B}(0\text{B},4\text{Si})$ borate tetrahedron has four silicate Q^4 units in its nearest environment, and $^{14}\text{B}(1\text{B},3\text{Si})$ tetrahedron $[\text{B}\text{O}_4]^-$, which is connected via bridging oxygen atoms to one similar tetrahedron and three fully polymerized silicate structural Q^4 units. The first configuration is typical of the reedmergnerite structure, and the second configuration is typical of

the danburite structure [27]. Data on the total integrated intensity (area) of resonance lines in ^{11}B NMR spectra measured by the authors of [33] are presented in Table 2. When interpreting the NMR spectroscopy data, it is generally accepted that the areas of individual resonance lines are proportional to the concentrations of their corresponding structural groups. It follows from the above that, at least at a qualitative level, the results of TD modeling can be compared with the values presented in Table 2.

Table 2. Total integrated intensity, A (sp. un.), resonant lines in ^{11}B NMR spectra of a number of sodium borosilicate glasses corresponding to the configurations $^{14}\text{B}(0\text{B},4\text{Si})$ and $^{14}\text{B}(1\text{B},3\text{Si})$. (The table was compiled according to the data of [33])

R	K		
	0.5	2	4
A			
0.25	0.163	0.176	0.192
0.5	0.319	0.377	0.373
0.75	0.329	0.514	0.533

According to the TD model (Fig. 14), the total concentration of danburite and reedmergnerite rings will increase with a change in the glass composition in the section with $R = 0.25$ in the direction from $K = 0.5$ to $K = 4$. However, such an increase will be quite small, since all three compositions of the experimentally studied glasses of this section are located near the same isoconcentration line. In glasses of the section with a constant ratio of sodium oxide to boron oxide of 0.5, the content of mixed borosilicate rings will also increase (much stronger than in the previous case) when K changes from 0.5 to 2, and then, when changing K from 2 to 4, a slight decrease in their concentration should be expected. An even stronger positive

increase in the concentration of danburite and reedmergnerite rings should be observed for the glasses of the section with $R = 0.75$ when K varies from 0.5 to 2. In this section, the further increase in the ratio of silicon oxide to boron oxide from 2 to 4 will not yield a significant change in the total concentration of borosilicate rings (the compositions of both glasses are located near 35% of the isoconcentration line). Referring to the data presented in Table 2, it is easy to see that the values of the areas of resonant lines given there change in a similar way. Hence it follows that the predictions of the TD model regarding the dependence of the content of mixed borosilicate rings on the composition in glasses of the $\text{Na}_2\text{O}-\text{B}_2\text{O}_3-\text{SiO}_2$ system do not contradict the experimental observations, at least qualitatively.

CONCLUSIONS

A comparative analysis of two known models of the structure of glasses in the $\text{Na}_2\text{O}-\text{B}_2\text{O}_3-\text{SiO}_2$ system on the scope and correctness (where possible) of the information they provide has been conducted. Both models provide comprehensive information on the distribution of basic structural units in glasses of various compositions, which is in good agreement with the experimental data available in the literature. Good agreement between the predictions of the Dell model regarding the dependence of the concentration of basic borate structural units on the glass composition is determined by its semiempirical nature. This also determines the simplicity of the mathematical formalism of the model, which, in fact, is a piecewise linear approximation of the distribution of the borate units actually existing in glasses. For the same reason, the predictive power of the Dell model is limited mainly by the local structure of the glass. In turn, the fundamental nature of the TD approach to modeling the structure and properties of oxide glasses provides a higher information content of the method, making it possible to obtain comprehensive information not only about the structure of glasses on near-order scales but also on their structure at the next hierarchical level, on intermediate-order scales. This is especially valuable due to the absence of quantitative experimental methods and techniques for determining the concentration of superstructural groups as a function of the glass composition. A qualitative comparison of the theoretical calculations of the distribution of superstructural groups in sodium borosilicate glasses with the experimental data showed the absence of any fundamental discrepancies between them.

CONFLICT OF INTEREST

The authors declare that they have no conflicts of interest.

REFERENCES

1. Wright, A.C., My borate life: An enigmatic journey, *Int. J. Appl. Glass Sci.*, 2015, vol. 6, no. 1, pp. 45–63.
2. Wright, A.C., Borate structures: Crystalline and vitreous, *Phys. Chem. Glasses: Eur. J. Glass Sci. Technol., Part B*, 2010, vol. 51, no. 1, pp. 1–39.
3. Dell, W.J., Bray, P.J., and Xiao, S.Z., ^{11}B NMR studies and structural modeling of $\text{Na}_2\text{O}-\text{B}_2\text{O}_3-\text{SiO}_2$ glasses of high soda content, *J. Non-Cryst. Solids*, 1983, vol. 58, pp. 1–16.
4. Feller, S., Mullenbach, T., Franke, M., Bista, S., O'Donovan-Zavada, A., Hopkins, K., Starkenberg, D., McCoy, J., Leipply, D., Stansberry, J., Troendle, E., Affatigato, M., Holland, D., Smith, M.E., Kroeker, S., Michaelis, V.K., and Wern, J.E.C., Structure and properties of barium and calcium borosilicate glasses, *Phys. Chem. Glasses: Eur. J. Glass Sci. Technol., Part B*, 2012, vol. 53, no. 5, pp. 210–218.
5. Maekawa, H., Maekawa, T., Kawamura, K., and Yokokawa, T., The structural groups of alkali silicate glasses determined from ^{29}Si MAS-NMR, *J. Non-Cryst. Solids*, 1991, vol. 127, pp. 53–64.
6. Osipov, A.A. and Osipova, L.M., Q^n distribution in silicates: Alkali silicate glasses and melts, *Adv. Mater. Res.*, 2012, vols. 560–561, pp. 254–258.
7. Osipov, A.A. and Osipova, L.M., New approach to modeling of a local structure of silicate glasses and melts, *J. Phys.: Conf. Ser.*, 2013, vol. 410, 012019.
8. Mysen, B.O. and Frantz, J.D., Raman spectroscopy of silicate melts at magmatic temperatures: $\text{Na}_2\text{O}-\text{SiO}_2$, $\text{K}_2\text{O}-\text{SiO}_2$ and $\text{Li}_2\text{O}-\text{SiO}_2$ binary compositions in temperature range 25–1783°C, *Chem. Geol.*, 1992, vol. 96, pp. 321–332.
9. Maehara, T., Yano, T., and Shibata, S., Structural rules of phase separation in alkali silicate melts analyzed by high-temperature Raman spectroscopy, *J. Non-Cryst. Solids*, 2005, vol. 351, pp. 3685–3692.
10. Malfait, W.J., Zakaznova-Herzog, V.P., and Halter, W.E., Quantitative Raman spectroscopy: Speciation of Na-silicate glasses and melts, *Am. Mineral.*, 2008, vol. 93, pp. 1505–1518.
11. Bykov, V.N., Osipov, A.A., and Anfilogov, V.N., Raman Spectroscopy of melts and glasses of the $\text{Na}_2\text{O}-\text{SiO}_2$ system, *Rasplavy*, 1998, no. 6, pp. 86–91.
12. Mysen, B.O. and Frantz, J.D., Silicate melts at magmatic temperatures: In situ structure determination to 1651°C and effect of temperature and bulk composition on the mixing behavior of structural units, *Contrib. Mineral. Petrol.*, 1994, vol. 117, pp. 1–14.
13. Schneider, J., Mastelaro, V.R., Zanotto, E.D., Shakhmatrin, B.A., Vedishcheva, N.M., Wright, A.C., and Panepucci, H., Q^n distribution in stoichiometric silicate glasses: Thermodynamic calculations and ^{29}Si high resolution NMR measurements, *J. Non-Cryst. Solids*, 2003, vol. 325, pp. 164–178.
14. Shakhmatkin, B.A. and Vedishcheva, N.M., A thermodynamic approach to modeling of physical properties of oxide glasses, *Glass Phys. Chem.*, 1998, vol. 24, no. 3, pp. 229–236.
15. Vedishcheva, N.M. and Wright, A.C., Chemical structure of oxide glasses: A concept for establishing structure-property relationships, in *Glass Selected Properties*

- and Crystallization*, Schmelzer, J.W.P., Ed., Berlin: De Gruyter, 2014, Chap. 5, pp. 269–299.
16. Vedishcheva, N.M., Shakhmatkin, B.A., and Wright, A.C., Thermodynamic modelling of the structure of sodium borosilicate glasses, *Phys. Chem. Glasses*, 2003, vol. 44, no. 3, pp. 191–196.
 17. Vedishcheva, N.M., Polyakova, I.G., and Wright, A.C., Short and intermediate range order in sodium borosilicate glasses: A quantitative thermodynamic approach, *Phys. Chem. Glasses: Eur. J. Glass Sci. Technol., Part B*, 2014, vol. 55, no. 6, pp. 225–236.
 18. Mishra, R.K., Sudarsan, V., Kaushik, C.P., Raj, K., Kulshretha, S.K., and Tyagi, A.K., Effect of BaO addition on the structural aspects and thermophysical properties of sodium borosilicate glasses, *J. Non-Cryst. Solids*, 2007, vol. 353, pp. 1612–1617.
 19. Nanba, T., Nishimura, M., and Miura, Y., A theoretical interpretation of the chemical shift of ^{29}Si NMR peaks in alkali borosilicate glasses, *Geochim. Cosmochim. Acta*, 2004, vol. 68, no. 24, pp. 5103–5111.
 20. Miyoshi, H., Chen, D., Masui, H., Yazawa, T., and Akai, T., Effect of calcium additive on the structural changes under heat treatment in sodium borosilicate glasses, *J. Non-Cryst. Solids*, 2004, vols. 345–346, pp. 99–103.
 21. Grandjean, A., Malki, M., Montouillout, V., Debruycker, F., and Massiot, D., Electrical conductivity and ^{11}B NMR studies of sodium borosilicate glasses, *J. Non-Cryst. Solids*, 2008, vol. 354, pp. 1664–1670.
 22. Martens, R. and Müller-Warmuth, W., Structural groups and their mixing in borosilicate glasses of various compositions—an NMR study, *J. Non-Cryst. Solids*, 2000, vol. 265, pp. 167–175.
 23. Winterstein-Beckmann, A., Moncke, D., Palles, D., Kamitsos, E.I., and Wondraczek, L., A Raman-spectroscopic study of indentation-induced structural changes in technical alkali-borosilicate glasses with varying silicate network connectivity, *J. Non-Cryst. Solids*, 2014, vol. 405, pp. 196–206.
 24. Michel, F., Cormier, L., Lombard, P., Beuneu, B., Galoisy, L., and Calas, G., Mechanism of boron coordination change between borosilicate glasses and melts, *J. Non-Cryst. Solids*, 2013, vol. 379, pp. 169–176.
 25. Fleet, M.E. and Muthupari, S., Coordination of boron in alkali borosilicate glasses using XANES, *J. Non-Cryst. Solids*, 1999, vol. 255, pp. 233–241.
 26. Osipov, A.A., Osipova, L.M., and Eremyashev, V.E., Structure of alkali borosilicate glasses and melts according to Raman spectroscopy data, *Glass Phys. Chem.*, 2013, vol. 39, no. 2, pp. 105–112.
 27. Manara, D., Grandjean, A., and Neuville, D.R., Advances in understanding the structure of borosilicate glasses: A Raman spectroscopy study, *Am. Mineral.*, 2009, vol. 94, pp. 777–784.
 28. Koroleva, O.N., Shabunina, L.A., and Bykov, V.N., Structure of borosilicate glasses according to Raman spectroscopy data, *Steklo Keram.*, 2010, no. 11, pp. 10–12.
 29. Furukawa, T. and White, W.B., Raman spectroscopic investigation of sodium borosilicate glass structure, *J. Mater. Sci.*, 1981, vol. 16, pp. 2689–2700.
 30. Windisch, C.F., Jr., Pierce, E.M., Burton, S.D., and Bovaird, C.C., Deep-UV Raman spectroscopic analysis of structure and dissolution rates of silica-rich sodium borosilicate glasses, *J. Non-Cryst. Solids*, 2011, vol. 357, pp. 2170–2177.
 31. Inoue, H., Masuno, A., and Watanabe, Y., Modeling of the structure of sodium borosilicate glasses using pair potentials, *J. Phys. Chem. B*, 2012, vol. 116, pp. 12325–12331.
 32. Gaafar, M.S. and Marzouk, S.Y., Mechanical and structural studies on sodium borosilicate glasses doped with Er_2O_3 using ultrasonic velocity and FTIR spectroscopy, *Phys. B (Amsterdam, Neth.)*, 2007, vol. 388, pp. 294–302.
 33. Du, L.-S. and Stebbins, J.F., Nature of silicon-boron mixing in sodium borosilicate glasses: A high-resolution ^{11}B and ^{17}O NMR study, *J. Phys. Chem. B*, 2003, vol. 107, pp. 10063–10076.